DOI: 10.65731/ama/2026-0070

WIND TUNNEL AND CFD STUDIES FOR DETERMINING FORCES ON A HYDROFOIL

Heiko MEIRONKE*, **Janusz A. SZYMCZYK****

*University of Applied Sciences Stralsund, Faculty of Mechanical Engineering,
Fluid Mechanics and Apparatus Engineering, Zur Schwedenschanze 15, 18435 Stralsund, Germany
**The Jacob of Paradies University, Department of Technology,
52 Fryderyka Chopina Street, Building 7, Gorzów Wielkopolski, 66-400, Poland

heiko.meironke@hochschule-stralsund.de, jszymczyk@ajp.edu.pl

received 20 January 2026, revised 26 July 2026, accepted 04 August 2026

Abstract: The subject of this paper is the investigation of the hydrodynamic properties of a wing combination of a hydrofoil system as a lift generating element of a foil board. The hydrofoil system consists of a main and a rear wing, which are connected by means of fuselage construction. This wing combination is attached below a foil board using a mast. As the forward motion accelerates, e.g., pumping, kite, sail, or electric motor, the board is gradually lifted out of the water and glides at a higher velocity due to the significantly reduced drag. The investigations are carried out using an existing hydrofoil system in a Göttingen-type wind tunnel. The wind tunnel tests are used to determine the forces and moments to describe the lift and drag behavior of the hydrofoil system. Numerical analyses were performed for the tests in wind tunnel and the results of the calculations were validated with the experimental results in air. In the following numerical simulations, the fluid air was replaced by water in order to obtain realistic data on the flow around a hydrofoil system. Similarity conditions between water and air flows were applied to define the relationship between different fluids and obtain realistic predictions of behavior at higher Reynolds numbers.

Key words: fluid dynamics, wind tunnel, hydrofoil, CFD

1. INTRODUCTION

In recent years, there has been a notable increase in the requirements for the development of energy-efficient and low-emission propulsion systems in the global maritime transport sector. This trend is closely linked to the European Union's climate targets for 2050, which demand comprehensive decarbonization of the maritime sector [1]. The main focus is on reducing energy consumption due to rising fuel costs, as well as reducing environmental pollution caused by highly polluting exhaust gases [2]. At the same time, interest is also growing in efficient solutions in the field of commercial shipping [3] and recreational boating in order to enable sustainable and efficient mobility. One technology that has gained increasing attention is the application of hydrofoils, which have been demonstrated to reduce energy consumption by up to 80% [4]. Particularly for smaller ferries operating in coastal areas, the drag reducing propulsion concept using hydrofoils is being researched and increasingly implemented [5]. The principle behind hydrofoils is that, once a certain speed is reached, the hull of a watercraft is lifted out of the water, thereby significantly reducing hydrodynamic drag. This effect is achieved by minimizing the wetted hull surface and shifting the primary drag to slender, optimized hydrofoils. The system acts as a lift generating element for a foil board, which may be powered by sail, electric propulsion, or human power.

Preliminary results from studies of a hydrofoil system were presented at the 2024 RET Conference [6]. Experimental investigations were conducted in a wind tunnel, followed by numerical simulations of this system in an airflow. The validation showed very good agreement between the experimental and numerical results.

The current study builds on the findings of the previous work, with the numerical simulation expanded to simulate the actual flow around the hydrofoil in water. The flow velocity in water is determined using similarity theory, and this flow velocity is then upscaled to the operating range of the hydrofoil system.

This resulted in a method for simulating the actual flow around a hydrofoil system in water using numerical simulations, based on the experimental wind tunnel tests.

2. EXPERIMENTAL AND NUMERICAL METHODS

The hydrofoil tests are carried out experimentally in a wind tunnel. Numerical analyses were performed for the tests and the results of the calculations were validated with the experimental results. Based on the results obtained from the numerical simulations of air flow in the wind tunnel, the flow around the hydrofoil system is then transferred to water, as hydrofoils are naturally used in the medium of water. Therefore, the similarity relationships between water and air flows must be taken into account in order to obtain realistic predictions of behavior at higher speeds in water. Flow phenomena in air and water are similar or analogous and can be related to each other in fluid mechanics using similarity theory. Differences, such as separation or cavitation, are not taken into account in the similarity relationships.

This theory is used in this study to link the experimental results in air with the numerical results in water.

The experiments and numerical simulations are carried out using an existing commercially available hydrofoil system. A three-dimensional geometric model is required for the flow simulation, which was created using 3D scanning and design methods (SolidWorks).

2.1. Experimental methods

The experimental investigations in this study were carried out in a Göttingen-type wind tunnel at the university Stralsund. The wind tunnel has a drive power of 45 kW and a measuring cross-section of 1000 mm x 1000 mm. With this measuring cross-section, flow velocities of up to 30 m/s can be achieved. The wind tunnel has an open measuring plenum in which the hydrofoil system was placed [7] (Fig. 1).

With the nozzle configuration used, the wind tunnel has a free-stream turbulence intensity of 0.15%. The effect of turbulence on the force measurements is roughly on the same order of magnitude as the measurement uncertainty of the force sensor.

The wind tunnel tests are used to determine the forces and moments caused by the flow in the x, y and z directions. The relationship between the lift force and the drag force plays a particularly important role. For systematic measurement of the forces, the angle of attack (AoA) is varied at different velocities in order to clearly describe the lift and drag behavior. The force in the x-direction F_x is assigned to the drag force F_D, the force in the y-direction F_y to the side force F_S, and the force acting in the z-direction F_z to the lift force F_L. In relation to the axes, these forces generate moments around the various axes.

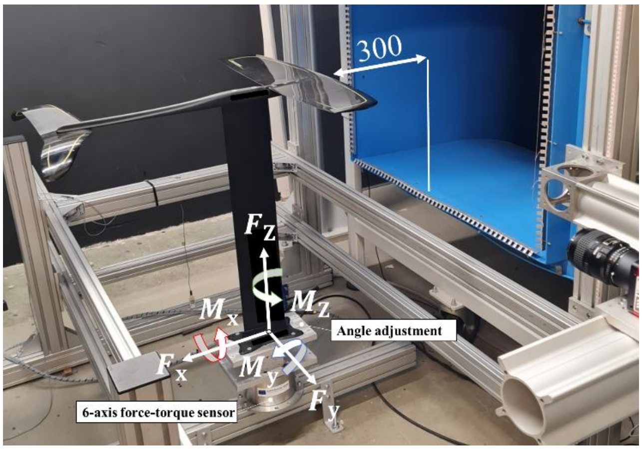

Fig. 1. Hydrofoil (overhead) mounted in the measuring plenum of the wind tunnel on the 6-axis force-torque sensor [7]

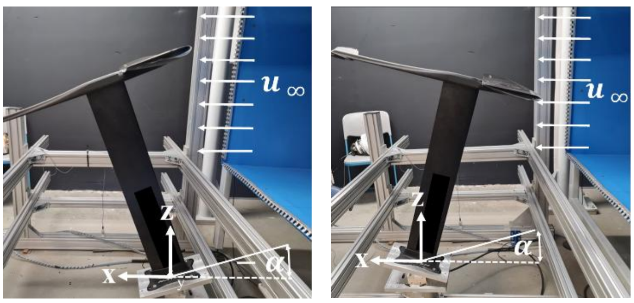

Fig. 2. Two different settings of hydrofoil with negative and positive angle of attack [7]

The hydrofoil system is installed upside down in the measurement plenum (rotated by 180°) for easier assembly and force/moment measurement.

The origin of coordinate system is located in the center of the contact plane of the sensor on which an adapter is installed (Fig.1). This adapter is used to adjust the angle of attack α of the hydrofoil. Figure 2 shows the experimental measurement setup with the hydrofoil system in the wind tunnel in a setup with negative and positive angle of attack. The positive angle of attack corresponds to the orientation of the hydrofoil system in the wind tunnel, where lift is generated. In contrast, a negative angle of attack generates negative lift (downforce).

The distance from the front wing to the nozzle outlet was set to 300 mm for each angle of attack α by moving it across the profile so that the measurements could be carried out under the same conditions. The measurement data was recorded using the same procedure. After setting the angle of attack in 1° increments from $-25° \leq \alpha \leq +25°$, the force and torque recording was started. All initial forces (weight) and moments were set to 0 and the flow velocity of the wind tunnel was set to 20 m/s. After reaching a steady state, all relevant measurement data, such as pressure, temperature and speed, as well as the forces and torques, were recorded at intervals of 0.5 seconds within 2 minutes and then averaged.

The forces and moments were measured using a 6-axis force-moment sensor “K6D154” from “ME Messsysteme GmbH” [8]. This paper focuses on force measurements. Torque measurements were not addressed in this paper.

The “K6D154” sensor has a measurement range of +/- 500 N for forces and +/- 50 Nm for torques. The sensor has an accuracy class of 0.2% FS, relative to the full-scale value (FS = Full Scale). This means that at +/- 500 N, an error of +/- 1 N would occur. Measurement uncertainties, such as zero-point drift, feedback, or installation errors, have been minimized as much as possible through careful preparation and multiple tests conducted in advance.

In particular, the experimental data on lift and drag forces are important variables that are used to determine the dimensionless coefficients. These coefficients are used to perform a general evaluation of the performance of the hydrofoil system at various settings, such as flow velocity at the nozzle outlet and angle of attack (AoA) [9].

2.2. Numerical methods

The numerical flow simulation was performed using the commercial software ANSYS-Fluent [7].

A hemispherical inflow region and a straight outflow region were created as the basic geometry of the three-dimensional flow space within the “DesignModeler” geometry tool.

The volume model around the airfoil was chosen to be large enough that its edges do not affect the flow around the hydrofoil system. This assumption also agrees, to a good approximation, with the experimental setup and the measurements, which correspond very well with the calculations. Any potential influence of the wind tunnel flow in the open measurement section on the hydrofoil system due, for example, to blockage, jet expansion, or jet deformation can be considered negligible given a blockage ratio of less than 10% and the positioning of the object (Fig. 1).

DOI: 10.65731/ama/2026-0070

The geometry of the hydrofoil system was embedded in this flow space geometry. A three-dimensional simulation is necessary to determine the inhomogeneous lift behavior over the entire foil surface as well as the tip vortices, which make a significant contribution to increasing drag. The spatial discretization of the flow domain (meshing) is the most complex part of the simulation. A high-quality computational mesh is essential for the reliability of the results, but its creation is a very time-consuming process.

The geometry data was used to create an unstructured mesh using "CFD Mesh" software. The creation of multiple zones within the mesh enabled local refinement of the mesh density and the creation of structured prismatic layers (inflation layers) in the boundary layer region.

A virtual zone (body of influence) was introduced in the area surrounding the hydrofoil system and due to the high pressure and velocity gradients in the wall-adjacent region in relation to the viscosity of the fluid, fine meshing is required in this region.

In addition, the mesh was further refined in the boundary layer with the goal of achieving a dimensionless wall distance of $y^+ \leq 1$.

Finer meshing of the boundary layer is also necessary in relation to the selected turbulence model, as there is not always a general wall function for the boundary layer profile [10]. The quality parameters, in particular those such as orthogonal quality (>0.8), skewness (<0.6), and growth rate (<1.2), were examined and showed good to very good values.

For symmetrical bodies, it is particularly useful to introduce a plane of symmetry to divide the object into two parts. Simulating one half of the model significantly reduces the necessary computing requirements and the calculation time.

Air at a constant density and a temperature of 20°C was defined as the fluid, since it is assumed to be an incompressible fluid.

The k-ω SST turbulence model was used to resolve the turbulent fluctuation movements, which is currently the optimal choice for flows with separations and stagnation points [11].

In this study, the simulation results are compared at different mesh densities to determine whether the solution stabilizes or continues to converge as the mesh becomes finer. The aim is to avoid a solution being dependent on the mesh resolution. Finally, a compromise is reached that provides a precise solution with moderate computational effort.

A simplified mesh independence study was conducted. For this purpose, the mesh was tested and compared in both the near-wall and far-wall regions using different element sizes. The target was to ensure that the deviation, e.g., in lift force, between the finer mesh and the coarser mesh was less than 2 %.

In the solver parameters, a convergence criterion of 10^{-3} was selected for all residuals. The number of iterations was set to n=200, since the convergence criterion was already met at n=190.

When setting the boundary conditions, it is particularly important to emphasize the variation in the angle of attack, especially with regard to the flow boundary condition at the inlet. In this case, the velocity is decomposed into the corresponding components in order to set the angle of attack α.

This smart method makes it possible to use only one geometry or mesh model without having to create special meshes with inclined wings. The turbulence intensity of the inlet flow was set to 0.15%, which corresponds to the free-stream turbulence intensity in the wind tunnel.

3. RESULTS AND DISCUSSIONS

3.1. Experimental Results

The forces and moments were measured in three spatial directions. The drag and lift forces are relevant for the performance of the hydrofoil system. Due to the symmetry of the geometry in the direction of flow, the side force ($F_S = F_y$ in Fig. 1) is of minor importance. The weight of the hydrofoil system is not taken into account in either experimental or numerical investigations.

Due to the overhead mounting of the hydrofoil system in the measurement section, negative lift forces are also generated at negative angles of attack α. Furthermore, the experimental and numerical results show that the values of the forces are not axisymmetric with respect to the y-axis. The reason for this is the asymmetrical profile of the front and rear wings, which have been optimized for lift and for positive angles of attack, respectively, to improve the performance of the foil board.

Figure 3 shows a representation of the measured forces in the respective coordinate directions ass a function of the angle of attack α, which can be used in particular for direct practical reference.

Figure 4 describes the dimensionless coefficients which play an important role in this representation for similarity mechanics and for direct comparison with the numerical results (see Fig. 5).

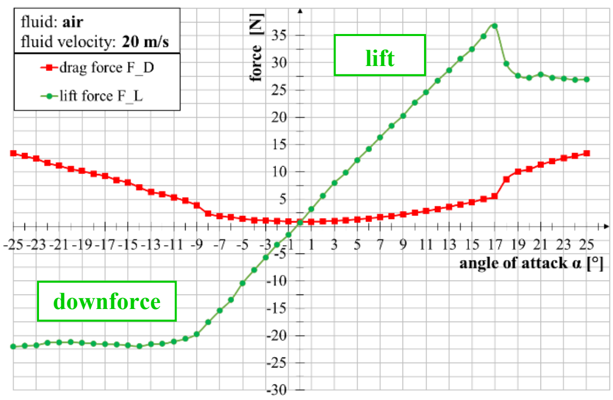

Fig. 3. Experimental data of forces from the wind tunnel as function of angle of attack α at a flow velocity of 20 m/s in air

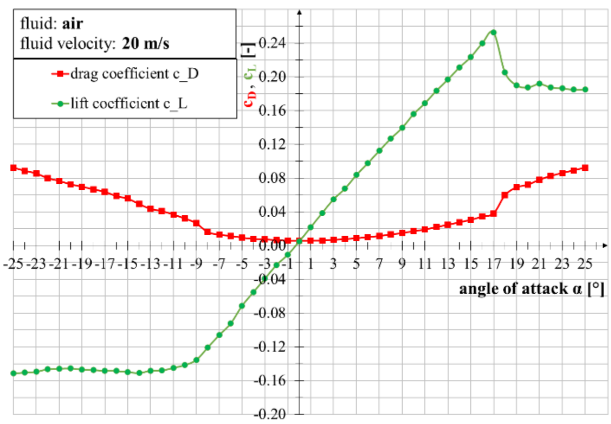

Fig. 4. Experimental data of coefficients from the wind tunnel as function of angle of attack α at a flow velocity of 20 m/s in air

The drag and lift coefficients were calculated from the force measurements of the "K6D154" sensor, the given area of the hydrofoil system, and the corresponding velocity (20 m/s) for various angles of attack (see formula 5).

This means that different fluids with different kinematic boundary conditions can be directly compared with each other at the same Reynolds numbers. The discussion of the curve trends is limited to positive angles of attack, as these ensure the function of the hydrofoil in practical use.

The negative angles of attack play a minor role in the operation of the board. These measured values are not considered further in this paper. An increase in the angle of attack (α) leads to a corresponding increase in the magnitude of the drag and lift forces.

It can be seen in Figure 3 that a minimum drag force of 0.87 N is achieved in the neutral position (0°). In terms of lift force, even in the neutral position there is a minimum lift of 0.7 N. The increase in resistance follows a slightly parabolic curve up to an angle of attack of approximately 17°. With increasing angle of attack, a significant increase in drag is observed, reaching approximately 14 N at an angle of attack of 25°.

The lift force increases almost linearly up to an angle of 17°. At this angle of attack, a maximum force of 36.8 N is reached. As the angle of attack increases, the lift force drops abruptly by approximately 10 N within 2°, resulting in a reduced lift force of 26.9 N at 25°. The significant change in drag and lift force in the region of the positive angle of attack range at 17° is associated with the separation of the boundary layer. The position of the separating boundary layer on the hydrofoil system shifts abruptly forward, leading to a sudden collapse of lift and increased drag (stall effect).

This limit state marks the maximum angle of attack of the hydrofoil system, which should not be exceeded without incurring a drastic loss of performance due to separation.

3.2. Validation of numerical results in air with experimental data in wind tunnel

Figure 5 shows the results of the experimental investigations regarding the lift and drag coefficients (Fig. 4) and the calculated values from the numerical simulation with the fluid air. The properties of air and the boundary conditions resulting from the experimental investigations in the wind tunnel were set as realistically as possible. The calculated results, in particular the forces and dimensionless coefficients, were adjusted to the full model based on the calculation with the symmetrical half model. The calculated results show a very similar pattern to the experimental results.

For each force component, we calculated the mean and the corresponding standard deviation based on 1,000 measurement values. In the paper, this mean value was used and presented for the validation.

The drag coefficient also increases significantly with increasing angle of attack, up to 0.084 at an angle of 25°. In the neutral position (0°), there is no lift coefficient, which indicates an excellent balance between the front wing and the stabilizing rear wing of the hydrofoil system. Increasing the angle of attack to 17° results in an almost linear increase in the lift coefficient to 0.24. A further increase in the angle of attack leads to a sudden drop in lift, which can be explained by the separation of the boundary layer (stall effect).

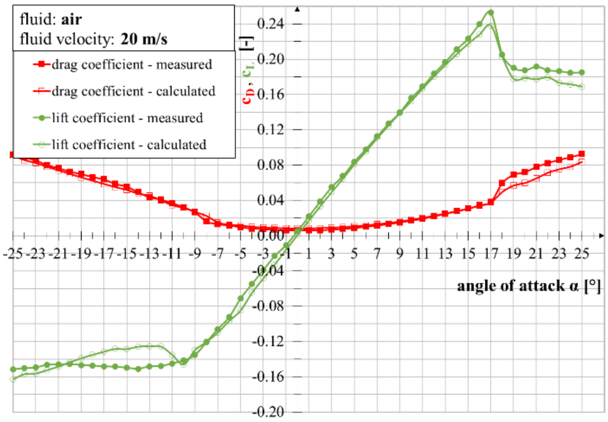

Fig. 5. Validation between experimental and numerical data at a flow velocity of 20 m/s in air

The drop occurs within a narrow angle range of 2° and then stabilizes at 19°–25° at a value between 0.17 and 0.18. A crucial procedure for ensuring the reliability of numerical simulations is the validation of the calculated data with experimental data. This process serves to confirm the accuracy and correctness of the selected methods and boundary conditions and to enable further reliable scaling or optimization of the geometry.

A comparison of the coefficients (Fig. 5) shows a high degree of agreement, especially for the drag coefficient, up to an angle of attack of 17°. At larger angles, boundary layer separation occurs. Here, the discrepancy between the calculated values and the experimental data increases significantly. This leads to a sharp increase in turbulence, large and transient vortices, and significant fluctuations in velocity in experimental and calculated results.

The correct setting of the turbulence model and the resolution of the mesh in the boundary layer are particularly important in the area of separation and strong vortex formation. This setting has a significant influence on the accuracy of the calculations. There is still a need for optimization in numerical simulation in this area.

3.3. Similarity conditions between air and water flow at the same Reynolds number

These investigations are characterized by the fact that the experimental tests were carried out in a wind tunnel, in a thinner medium of air, whereas the actual flow around a hydrofoil system naturally takes place in a much denser medium of water. This requires the consideration of similarity relationships and the determination of a physical similarity between the flow conditions. Similarity theory states that the flow conditions or flow behavior in different systems are similar if the dimensionless parameters are the same [12, 13].

This presupposes that the ratio of inertial forces to frictional forces must be the same in the model as in the original. This interaction is determined by the Reynolds number.

This means that in this case, the Reynolds numbers (*Re*) for air Re_{air} and water Re_{water} must be the same:

$$Re_{air} = Re_{water} \tag{1}$$

with equation (1) follows:

$$\frac{\rho_{air} \cdot u_{air} \cdot L}{\eta_{air}} = \frac{\rho_{water} \cdot u_{water} \cdot L}{\eta_{water}} \tag{2}$$

 DOI: 10.65731/ama/2026-0070

resolved with respect to velocity u_{water}:

$$u_{water} = \left(\frac{\eta_{water}}{\eta_{air}}\right) \cdot \left(\frac{\rho_{air}}{\rho_{water}}\right) \cdot u_{air} \tag{3}$$

applied with the properties for air and water at a temperature $T = 20°C$ and an ambient pressure of $p_a = 1\ bar$, which are also used in the simulation, the result is:

$$u_{water} = \frac{1.003 \cdot 10^{-3}}{1.7894 \cdot 10^{-5}} \cdot \frac{1.225}{998.2} \cdot 20 \frac{m}{s} = \frac{1}{14.537} \cdot 20 \frac{m}{s}$$
$$u_{water} = 1.376 \frac{m}{s} \tag{4}$$

A flow velocity of $u_{water} = 1.376 \frac{m}{s}$ in water corresponds to a flow velocity of $u_{air} = 20 \frac{m}{s}$ in air according to equation (4).

Table 1 compares the results from the numerical simulations with these two velocities and angles of attack of $\alpha = 10°$ and $\alpha = 20°$.

Tab. 1. Comparison of the numerical results of air and water flow at same Reynolds numbers and at two different angles of attack

	air ($u_{air} = 20$ m/s)		water ($u_{water} = 1.376$ m/s)	
	$\alpha = 10°$	$\alpha = 20°$	$\alpha = 10°$	$\alpha = 20°$
drag force F_D [N]	2.6210	9.468	10.0980	36.5410
drag force coefficient c_D [-]	0.0180	0.0651	0.0180	0.0651
lift force F_L [N]	22.1670	25.985	85.5460	100.2180
lift force coefficient c_L [-]	0.1525	0.1787	0.1524	0.1787

The factors determined from the numerical simulation can be compared with those from the theoretical consideration of similarity relationships. The following relationships apply to the drag forces in water and air:

$$F_{D\,(water)} = c_{D\,(water)} \cdot \frac{\rho_{water}}{2} \cdot u_{water}{}^2 \cdot A \quad \text{and}$$
$$F_{D\,(air)} = c_{D\,(air)} \cdot \frac{\rho_{air}}{2} \cdot u_{air}{}^2 \cdot A \tag{5}$$

The same Reynolds numbers for water and air flow indicate that the drag coefficients must also be the same.

$$c_{D\,(water)} = c_{D\,(air)} \tag{6}$$

$$\frac{F_{D\,(water)}}{F_{D\,(air)}} = \frac{c_{D\,(water)} \cdot \frac{\rho_{water}}{2} \cdot u_{water}{}^2 \cdot A}{c_{D\,(air)} \cdot \frac{\rho_{air}}{2} \cdot u_{air}{}^2 \cdot A}$$
$$\frac{F_{D\,(water)}}{F_{D\,(air)}} = \frac{944.98\ N}{245.00\ N} = 3.857 \tag{7}$$

It can be seen that the drag force, e.g., at an angle of attack of 10°, is in a ratio of 1 to 3.8527 and the lift force is in a ratio of 1 to 3.8592. Similar factors apply at an angle of attack of 20°.

In summary, it can be stated that, due to the ratio of the kinematic viscosities between air and water, a scaling factor for the velocity of 14.537 results under the given conditions with regard to the required equality of the Reynolds number. This implies that a real flow velocity of 1.376 m/s around the hydrofoil system in water corresponds to a flow velocity of 20 m/s in the wind tunnel. In terms of the forces and moments acting, this results in a scaling factor of 3.857. Assuming a constant Reynolds number, this results in a flow angle of attack of 10° for the analyzed hydrofoil system, with a lift force of 22.167 N in air, but a lift force of 85.546 N in water (Table 1).

3.4. Numerical Results in water

In the following numerical investigations, the fluid air was replaced by water in order to obtain realistic data on the flow around a hydrofoil system. As a further new boundary condition resulting from the similarity considerations outlined in Section 3.3, the velocity was adjusted to the corresponding range. Numerical calculations were performed for speeds of 1 to 5 m/s, and the coefficients and forces are shown in Figures 6 and 7. The possibility of extensive cavitation was examined. At the given flow velocities, with a flow velocity in water of up to 5 m/s, surface cavitation is not expected to occur.

The numerical results in water show very good agreement with the results in air flow, especially in the range up to an angle of attack of 15°, as they are mechanically similar. It can be seen that there is no dependence on the Reynolds number and that an almost linear progression of the lift force occurs with increasing angle of attack. This relationship has already been observed in research by Abbott and von Doenhoff [14] and Brunner et al. [15] and has been confirmed by the present study.

Despite mechanical similarities, there are differences in water, especially at increasing angles of attack. In water, even at low Reynolds numbers (see Fig. 6, Re = 100,000), there is a significant decrease in lift at an angle of attack (AoA) of 15°. At higher Reynolds numbers, it can be seen that the range in which the lift force begins to decrease shifts toward larger angles of attack. This relationship is due to the separation of the boundary layer, whose separation range shifts toward the trailing edge of the hydrofoil.

The asymmetrical geometry of the hydrofoil results in different behavior when it is set at a positive or negative angle. With a positive angle of attack, a significantly larger range of angles is available for lift, thus achieving a higher lift coefficient. In practice, the negative angle of attack is not particularly important, but rather serves to moderate the foil board's lift during the transition to the acceleration phase.

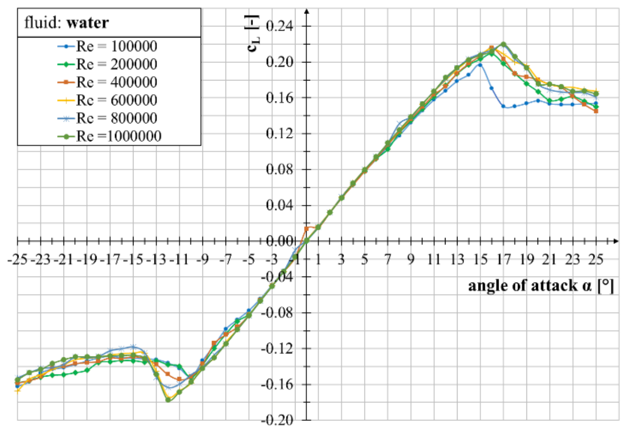

Fig. 6. Lift coefficients as a function of AoA for different Re numbers in water

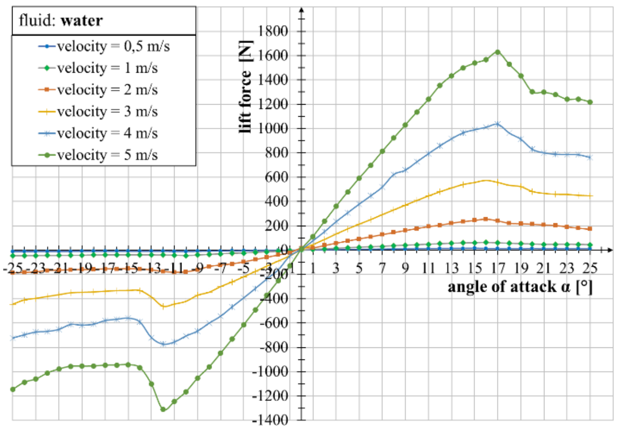

Fig. 7. Lift forces as a function of AoA for different velocities in water

Figure 7 shows important data for practical application. Depending on the angle of attack and the flow velocity, the forces required to operate a hydrofoil can be determined directly.

For example, a larger angle of attack is required when starting up in order to achieve maximum lift at low speeds. As the speed increases, the angle of attack must be gradually reduced to reduce the stress on the hydrofoil system and the drag. Furthermore, a reduction in the angle of attack is necessary to avoid stall, which would cause the lift force to collapse. It can be seen that, for example, at an angle of attack of 16° at a speed of 2 m/s, a lift force of approx. 250 N is generated, which would lift the board slightly out of the water during the start-up phase. In contrast, at an angle of attack of 9° and a speed of 5 m/s, a lift force of approx. 1000 N is generated, which represents a good operating point in riding mode.

Figure 8 shows the course of the drag coefficient as a function of the angle of attack for different Re numbers. Here, an almost identical course can be seen for all Re numbers investigated up to a positive angle of attack of 15°. As the angle of attack increases further, a significantly more diffuse behavior can be seen, which is due to the separation of the boundary layer. The detached boundary layer causes additional drag to be induced in the flow due to the turbulent flow.

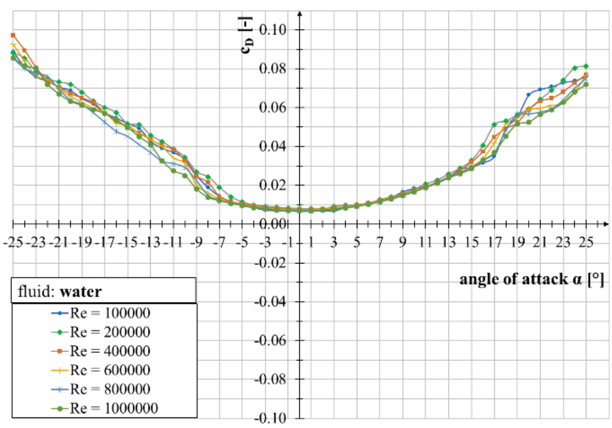

Fig. 8. Drag coefficients as a function of AoA for different Re numbers in water

Figure 9 shows the drag forces for different velocities as a function of the angle of attack. This representation of the drag behavior in dimensional form allows a direct assignment of the variables, which is particularly important for practical applications and, for example, provides a direct correlation with the required propulsion power.

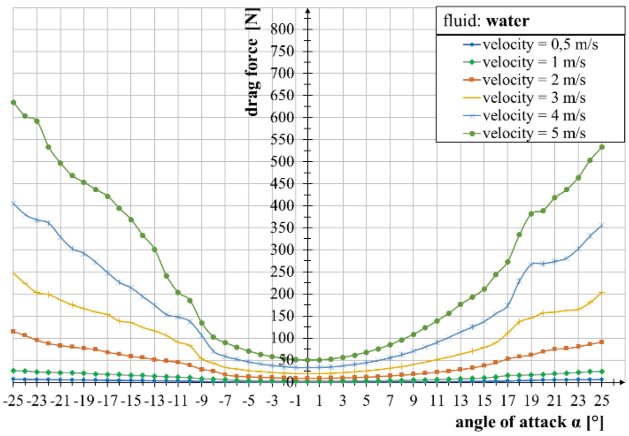

Fig. 9. Drag forces as a function of AoA for different velocities in water

It can be easily proven that the drag of the hydrofoil system increases quadratically with increasing speed at the same angle of attack. For example, at an angle of attack of 12°, the drag increases by a factor of four from 25 N to 100 N when the speed is doubled (from 2 m/s to 4 m/s). Under ideal conditions, doubling the speed of the hydrofoil system would result in an eightfold increase in the power that would have to be provided by the propulsion system.

4. CONCLUSIONS

This paper investigates the aero-/hydrodynamic properties of a hydrofoil system with the aim of analyzing the lift and drag forces and their dependence on the angle of attack and flow velocity. The investigations were carried out using an existing commercially available hydrofoil system consisting of a front wing, a stabilizing rear wing, a connecting fuselage, and a mast connecting the hydrofoil system to the board.

Comprehensive experiments were conducted in a wind tunnel with the aim of determining the forces in the x, y, and z directions on the three axes. The experimental tests were carried out in a Göttingen-type wind tunnel at the University of Stralsund [7], which has a drive power of 45 kW and a nozzle cross-section of 1000 mm x 1000 mm. This allows air flows of up to 30 m/s to be generated in the open measurement plenum (Fig. 1). Lift and drag were of particular importance in the measurements, as these variables are crucial for the function and evaluation of the performance of the hydrofoil system.

The minimum drag force of 0.87 N occurs at the neutral position (0°) and increases along a slightly parabolic trend up to an angle of attack of approximately 17°, followed by a steeper rise to about 14 N at 25°. The lift force is already 0.7 N at 0° and increases almost linearly, reaching a maximum of 36.8 N at an angle of attack of approximately 17°. At angles of attack greater than about 17°, increasing flow separation causes a stall, resulting in a significant loss of lift. (Fig. 3).

The experimental results in the air flow were validated using numerical flow simulations (Fig. 5). The results of the flow simulation were in good agreement with the experimental data, which confirmed the accuracy of the numerical models and boundary conditions. These models were then applied to the water flow to simulate the real operating conditions of a hydrofoil system.

DOI: 10.65731/ama/2026-0070

Similarities between water and air flows were important in achieving realistic predictions of behavior at higher velocities. The numerical results in the water flow show very good agreement with the results in the air flow, especially in the range up to an angle of attack of 15°, as they are mechanically similar. It can be seen here that there is no dependence on the Reynolds number and that an almost linear behavior of the lift force occurs with increasing angle of attack (Fig. 6). Despite mechanical similarity, however, there are differences in water, especially at large angles of attack (AoA>15°). Here, for example, as the Reynolds number increases, the range in which the lift force decreases dramatically (stall range) shifts toward larger angles of attack. This enables the hydrofoil system to increase lift force as the angle of attack increases, while keeping it almost stable to prevent flow separation. However, at the same time, the drag and thus the power required to run the system also increases significantly.

There is potential for optimization in the creation of the geometric model, as it can only be reproduced approximately due to the free-form surfaces in the original. This can lead to minimal deviations in shape compared to the original, which in turn can lead to slight differences in the calculated forces and in the position of the boundary layer separation line.

In further investigations, profiles with similar aerodynamic or hydrodynamic behavior will be simulated experimentally and numerically in order to further improve the experimental and numerical methods and refine the accuracy of the numerical simulation. In addition, experiments are planned to visualize the adjacent flow and the separations of the boundary layer. Regarding future research, we plan to conduct extensive studies in a towing tank.

REFERENCES

1. Istrate IR, Iribarren D, Dufour J, Ortiz Cebolla R, Arrigoni A, Moretto P, Dolci F. Quantifying emissions in the European maritime sector. JRC technical report; 2022.
2. Bai J, Yan Y, Bai X. A comprehensive review of ship emission reduction technologies for sustainable maritime transport. Frontiers in Marine Science. 2025;12.
3. Hüffmeier J, Johanson M. State-of-the-Art Methods to Improve Energy Efficiency of Ships. Journal of Marine Science and Engineering. 2021; 9: 447.
4. Köhler J, Graff E. Studie „Emissionsarme Antriebsarten auf dem Wasser – Zukunftsperspektiven“. Fraunhofer Institut ISI. Karlsruhe; 2025.
5. Godø JMK, Steen S, Faltinsen OD. A resistance model for hydrofoil fast ferries with fully submerged foil systems. Ocean Engineering. 2024; 301: 117503.
6. Meironke H, Panten T, Strubel F. Investigation of fluid dynamic properties of a hydrofoil wing combination using experimental and numerical methods. 26nd International Symposium “Research-Education-Technology”. ISBN: 978-3-911138-02-4. Stralsund. 2024; 142-149.
7. Strubel F. Bestimmung von strömungsmechanischen Parametern einer Flügelkombination eines Hydrofoils mittels numerischer und experimenteller Methoden. Master thesis. University of Applied Sciences Stralsund; 2023.
8. ME-Meßsysteme GmbH. Datenblatt Mehrkomponenten-Sensor K6D. Henningsdorf; 2023.
9. Martinez-Barbera H et al. Fluid Forces on a Hydrofoil for Kite- and Windfoil Boards. Journal of Marine Science. 2026; 25.
10. Menter FR, Matyushenko A. Best Practice: RANS Turbulence Modeling in ANSYS CFD. ANSYS Report; 2021.
11. Alonso LJ, Calderon-Sanchez J. Parametric design of hydrofoils. Ocean Engineering. 2025;318:120058.
12. Prandtl L, Tietjens OG. Applied Hydro- and Aeromechanics: Based on Lectures of L. Prandtl. McGraw-Hill Book Company; 1934.
13. Zierep J. Ähnlichkeitsgesetze und Modellregeln der Strömungslehre. Karlsruhe: Braun-Verlag; 1991.
14. Abbott IH, von Doenhoff AE. Theory of Wing Sections: Including a Summary of Airfoil Data. New York: Dover Publications; 1959.
15. Brunner CE, Kiefer J, Hansen MOL, Hultmark M. Study of Reynolds number effects on the aerodynamics of a moderately thick airfoil using a high-pressure wind tunnel. Experiments in Fluids. 2021;62:178.

The authors gratefully acknowledge the financial support by European Union – European Regional Development Fund (ERDF) for the financial support of the wind tunnel and measurement instruments (FHHST 10).

EUROPEAN UNION
European Regional Development Fund

Heiko Meironke: https://orcid.org/0000-0002-4808-1300

Janusz A. Szymczyk: https://orcid.org/0000-0003-4292-0529